On the Importance of High–Fidelity Numerical Modelling of Ocean Wave Energy Converters under Controlled Conditions

Materials Research Proceedings **20** (2022) 31-38 https://doi.org/10.21741/9781644901731-5

On the Importance of High–Fidelity Numerical Modelling of Ocean Wave Energy Converters under Controlled Conditions

Christian Windt[1*], Josh Davidson[2], Nicolas Faedo[1], Markel Penalba[3] and John V. Ringwood[1]

[1]Centre for Ocean Energy Research, Maynooth University North Campus, Maynooth, Co. Kildare, Ireland

[2]Department of Fluid Mechanics, Faculty of Mechanical Engineering Budapest University of Technology and Economics, Budapest, Hungary

[3]Department of Mechanical Engineering and Industrial Production Mondragon Unibertsitatea, Mondragon, Pais Vasco, Spain

[*]e-mail: christian.windt.2017@mumail.ie

Keywords: Wave Energy Converter, Numerical Modelling, BEM, CFD, Control

Abstract. Numerical modelling tools are commonly applied during the development and optimisation of ocean wave energy converters (WECs). Models are available for the hydrodynamic wave structure interaction, as well as the WEC sub–systems, such as the power take–off (PTO) model. Based on the implemented equations, different levels of fidelity are available for the numerical models. Specifically under controlled conditions, with enhance WEC motion, it is assumed that non-linearities are more prominent, re- quiring the use of high–fidelity modelling tools. Based on two different test cases for two different WECs, this paper highlights the importance of high–fidelity numerical modelling of WECs under controlled conditions.

Introduction

The growing recognition of human induced global warming has fuelled the research and development (R&D) of novel technologies to harness renewable energy resources. Amongst these resources, marine renewable energy, and specifically ocean wave energy, shows significant potential to contribute to the global energy supply [1]. To increase the efficiency and, thereby, the economical feasibility of WECs, devices should be equipped with energy maximising control systems (EMCSs) [2]. Since the objective of EMCSs is to drive the system towards resonance with the incoming wave field, WEC motion of a controlled device is enhanced (see Figure 1), and the power conversion is increased.

During the design and optimisation of WECs, researchers and engineers rely on physical wave tank (PWT), as well as numerical wave tank (NWT) tests. Generally, by testing in a real physical environment, PWTs allow all the relevant details of the wave-structure interaction (WSI) to be captured. However, although still cheaper compared to open ocean trials, PWT experiments are associated with higher costs compared to NWT experiments [3]. The main cost drivers for PWT tests are instrumentation, construction of the prototype, test facilities, and staff. Additionally, the accuracy of PWT experiments potentially suffer from peculiarities of the test facility, such as reflections from the tank walls, friction in mechanical device components, measurement noise, and scaling effects.

Materials Research Proceedings **20** (2022) 31-38 https://doi.org/10.21741/9781644901731-5

Overcoming the drawbacks of high costs, measurement noise, mechanical friction, and, to a great extent, scaling effects, NWTs provide powerful tools for the analysis of WECs. Depending on the implemented equations for the solution of the WSI problem, different levels of fidelity, at different levels of computational cost, can be achieved [4]. Hydrodynamic, lower-fidelity models, such as Boundary Element Method (BEM) - based NWTs, neglecting non-linear effects, such as viscosity, are associated with minimal computational cost, and are valuable tools for parametric studies or exhaustive-search optimisation algorithms. However, due to the required linearisation of the hydrodynamic equations, lower-fidelity models are only valid when considering linear conditions, i.e. small amplitude waves and device motions. Contrary, higher-fidelity NWTs, such as Computational Fluid Dynamics (CFD)-based numerical wave tanks (CNWTs), are able to capture all relevant hydrodynamic non-linearities by numerically solving the Navier-Stokes equations. Thus, CNWTs are valid over a wider range of test conditions, compared to lower-fidelity models.

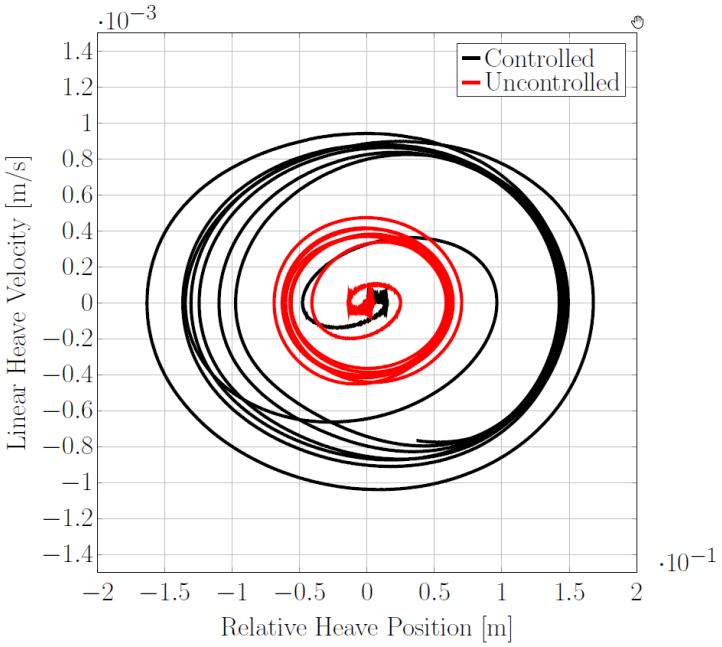

Figure 1: Operation space of uncontrolled and controlled WEC devices under regular wave excitation.

Equally, when considering the sub–systems of a WEC device, such as the power–take off (PTO) or the mooring system, a range of numerical models with varying degree of fidelity are available and can be coupled with the hydrodynamic model [5]. Generally, the implementation of high–fidelity models of the WEC sub–systems is desired when employing CNWTs, to prevent the lower–fidelity sub–system models from undermining the accuracy of the high–fidelity hydrodynamic model.

The importance of high–fidelity modelling of the WSI, as well as the WEC sub–system, specifically under controlled conditions, will be investigated in the present paper. To that end, two different case studies are considered, analysing two different WECs: (1) the Wavestar device; (2) a generic heaving point absorber (HPA) type WEC (see Figure 2). In the first case study, considering the Wavestar device, the influence of different design and evaluation frameworks for EMCSs will be investigated, employing three different EMCSs of varying *aggressiveness*. In the second case study, considering the HPA-type WEC, the influence of the fidelity of the hydrodynamic model and the coupled PTO model is investigated.

The remainder of the paper is organised as follows: Section 2 details the low– and high– fidelity numerical wave tanks employed in the two case studies. Furthermore Section 2 presents a description of the employed PTO models. The results of the first case study, assessing the evaluation framework of EMCSs, will be presented and discussed in Section 3.

The second case study, investigating the influence of the fidelity of the hydrodynamic and PTO model, is discussed in Section 4. Finally, conclusions are drawn in Section 5.

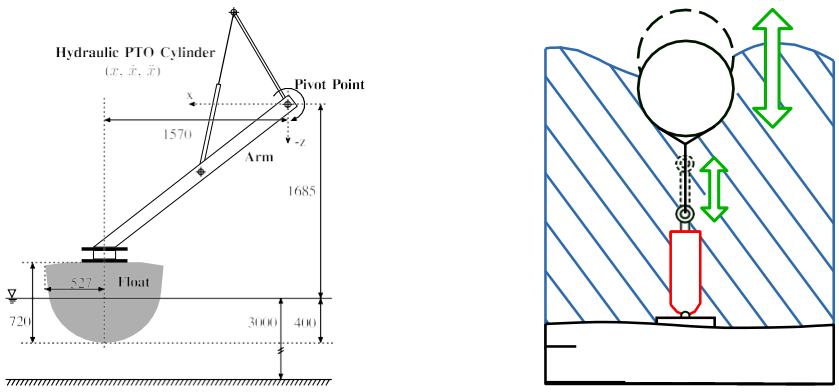

(a) (b)

Figure 2: The considered WECs: (a) the Wavestar device; (b) a generic heaving point absorber (HPA) type WEC

Numerical of WECs

BEM-based NWTs (BNWTs). Linear time-domain hydrodynamic models based on the BEM use, in general, Cummins equation [6], following:

$$M\ddot{x}(t) = -s_h x + \mathcal{F}_{exc}(t) - \mu_\infty \ddot{x}(t) - \int_{-\infty}^{\infty} K_{rad}(t-\tau)\dot{x}(\tau)d\tau + u(t), \quad (1)$$

where x, $\dot{x}$ and $\ddot{x}$ are the displacement, velocity and acceleration of the WEC, respectively. M is the mass of the WEC, s_h the hydrostatic stiffness, $\mathcal{F}_{exc}(t)$ the excitation force, μ_∞ the added-mass at infinite frequency, ζ(t) the radiation impulse response function (IRF), and $u(t)$ the control law (PTO force).

The linear hydrodynamic model can be extended to include non–linear effects, such as nonlinear Froude–Krylov (FK) forces or viscous effects. Non–linear FK forces can be included using, e.g. the computationally efficient algebraic solution as presented in [7]. Viscous effects can be incorporated by using a Morison-like equation [8],

$$F_{visc} = -\frac{1}{2}\rho C_d A_d(t)|\dot{z_d} - \dot{\eta}|(\dot{z_d} - \dot{\eta}), \quad (2)$$

where ρ is the density of water, C_d the drag coefficient, A_d the instantaneous cross-sectional area of the device, and $\dot{\eta}$ the velocity of the undisturbed water particles.

CNWT. The CNWT simulations are performed using the open source CFD toolbox Open-FOAM. In OpenFOAM, the incompressible Reynolds Averaged Navier-Stokes (RANS) equations (3) and (4) are solved using the finite volume method.

$$\nabla \cdot \rho \boldsymbol{U} = \boldsymbol{0} \quad (3)$$

$$\frac{\partial(\rho U)}{\partial t} + \nabla \cdot (\rho UU) = -\nabla p + \nabla \cdot T + \rho f_b \quad (4)$$

Equation (3) is the continuity equation, describing the conservation of mass, and equation (4) is the momentum equation. describing the conservation of momentum. In equations (3) and (4), $\boldsymbol{U}$

denotes the fluid velocity, p the fluid pressure, ρ the fluid density, T the stress tensor, and $\boldsymbol{f_b}$ external forces such as gravity or PTO forces.

To account for the two phase flow, the volume of fluid method, proposed in [9], is used, following:

$$\frac{\partial \alpha}{\partial t} + \nabla \cdot (u\alpha) + \nabla \cdot [u_r \alpha(1-\alpha)] = 0 \tag{5}$$

$$\Phi = \alpha \Phi_{\text{water}} + (1-\alpha)\Phi_{\text{air}} \ , \tag{6}$$

where α denotes the volume fraction of water, $\boldsymbol{u_r}(t)$ is the relative velocity between the liquid and gaseous phases [10], and Φ is a specific fluid quantity, such as density. The free surface elevation is monitored by extracting the iso-surface of the volume fraction $\alpha = 0.5$.

PTO. As for the hydrodynamic model, different levels of fidelity are available for the modelling of the PTO system of a WEC. One of the simplest models describes the PTO as a spring damper system, following:

$$F_{\text{PTO}}(t) = Kx(t) + B\dot{x}(t) \tag{7}$$

where B is a damping coefficient and $\dot{x}(t)$ the linear velocity of the hydraulic PTO cylinder, K is a spring stiffness, and $x(t)$ the linear motion of the PTO. The damping and stiffness coefficient either represent the mechanical characteristics of, say, a hydraulic cylinder, or B and K are representing the EMCSs and are optimised for maximum energy absorption. Higher–fidelity PTO models are available, including e.g. a hydraulic transmission system and an electrical generator [11]. The mathematical model for the hydraulic cylinder may include end-stop constraints, friction losses, and compressibility and inertia effects, providing the final PTO force, following:

$$F_{PTO} = A_p \Delta p + F_{fric} + F_I \tag{8}$$

where A_p is the piston area, Δp the pressure difference between the different cylinder chambers, F_{fric} the friction force and F_I the inertia force. For a detailed description of the individual effects, influencing the PTO force, the interested reader is referred to [11].

Case study 1: Assessment of the evaluation framework for EMCSs

In classical control applications, the mathematical models, used for the controller design, are often linearised around a desired operational point, according to the process under analysis. The controller is subsequently synthesised to drive the system towards this point and, thus, in the neighbourhood of this operational point, the linearising assumption is obeyed. The large amplitude motions, induced by a reactive WEC controller, may result in viscous drag and other non-linear hydrodynamic effects. Thus, contrary to the aforementioned classical control applications, the energy-maximising operating conditions do not comply with the linear assumption in the control design model.

This contradiction between the control objective and the underlying mathematical model raises the question if the common practice of designing a controller in a linear design environment can deliver optimal reactive controllers for the application in physical, non-linear operational conditions.

In this case study, a CNWT and linear BNWT model[1], as described in Section 2, are employed to investigate the influence of different numerical evaluation frameworks on the performance

[1] Note that, for this case study, any non-linearities, such as non-linear FK forces or viscous drag effects, are neglected.

evaluation of EMCSs for the Wavestar device (see Figure 2a). The performance of the EMCSs will be evaluated by comparing the dynamics of the WEC subject to three different EMCSs: (1) moment-based energy-maximising control [12]; (2) reactive output feedback control; (3) resistive output feedback control.

The three EMCSs will drive the WEC away from the linear assumption in the hydrodynamic model, dependent on the aggressiveness of the controller, with the resistive controller being the least aggressive and the moment-based control the most aggressive.

EMCSs. The main objective of a wave energy device is to harvest energy from the incoming wave field. Therefore, the optimal control objective is to maximise the absorbed energy over a time interval [t, t + T], while respecting the physical limitations of the device/PTO on excursion $x(t)$, velocity $\dot{x}(t)$, and PTO force $u(t)$. Consequently, the optimal control objective can be formulated as

$$u^{\max}(t) = \arg\max_{u(t)} \int_t^{t+T} u(\tau)\dot{x}(\tau)d\tau \tag{9}$$

The optimal control is a moment-based WEC formulation [12] which allows an efficient computation of the optimal control law $u^{\max}$ in real-time based on the solution of the following inequality constrained quadratic program:

$$L_u^{\max} = \arg\max_{L_u} -\frac{1}{2}L_u\Phi_{\varphi}^{\mathcal{R}}L_u^{\top} + \frac{1}{2}L_{exc}\Phi_{\varphi}^{\mathcal{R}}L_u^{\top}, \tag{10}$$

The reader is referred to [12] for the formal definition (and corresponding proofs) of the matrices involved in the QP problem of (10).

Additionally to the moment-based controller, less aggressive EMCSs, i.e. reactive and resistive controllers, are considered herein. For the reactive control case, the PTO force follows

$$u(t) = K_{\text{opt}}x(t) + B_{\text{opt}}\dot{x}(t) \tag{11}$$

where B_{opt} is the optimal damping coefficient and K_{opt} is the optimal spring stiffness. The optimal PTO coefficients have been determined through exhaustive search optimisation using the BNWT model. For the resistive control case, only the second term, $B_{\text{opt}}\dot{x}(t)$, is considered. As in the case of reactive control, the optimal damping coefficient has been determined through exhaustive search optimisation using the BNWT model.

Results. For each EMCSs, simulations were performed in the BNWT and CNWT, resulting in a total of six simulations. Extracting the PTO displacement, velocity, and the PTO force, the normalised root mean squared deviation (nRMSD), as defined in equation (12), can be calculated. y_{BNWT} denotes the results from the BNWT experiment, y_{CNWT} results from the CNWT experiment, and N is the number of samples.

$$\text{nRMSD} = \sqrt{\frac{\sum(y_{\text{CNWT}}-y_{\text{BNWT}})^2}{N}} \cdot \frac{1}{\max(y_{\text{BNWT}})-\min(y_{\text{BNWT}})} \cdot 100\% \tag{12}$$

For a qualitative comparison between the three different EMCSs, Figure 3 shows the PTO displacement, extracted from the BNWT experiment. In Figure 3, a clear trend can be observed.

Materials Research Proceedings **20** (2022) 31-38 https://doi.org/10.21741/9781644901731-5

The moment-based and the reactive controller controller increases the PTO displacement, compared to the resistive controller.

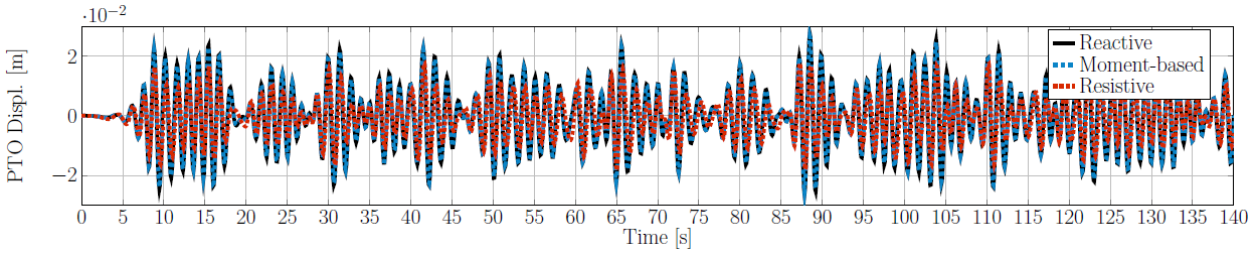

Figure 3: Time traces of the PTO displacement x(t) from the BNWT experiment

The resulting nRMSD for the PTO displacement, velocity, and force are listed in Table 1. Overall smallest values of the nRMSD can be observed for the case of a resistively controlled device. For this control strategy, smallest deviations are indeed expected, since the device effectively acts as a wave follower, reducing the influence of non-linear hydrodynamic effects, such as non-linear Froude-Krylov forces or viscous drag effects.

For the cases with reactive and moment-based control, the values for the nRMSD in all PTO quantities increase. In Table 1, it can be seen that the differences between the PTO quantities for the two different controllers are relatively small. This can be attributed to the fact that both state (displacement) and input (PTO force) constraints are inactive for this particular input wave, i.e. both controllers effectively reflect the unconstrained optimal energy-absorption conditions. That said, it is expected that also the differences between the BNWT and CNWT are similar.

Table 1: nRMSD between the results for PTO cylinder displacement, velocity and PTO force from the BNWT and CNWT for the different EMCSs

nRMSD [%]		Moment-based	Reactive	Resistive
PTO cylinder displacement	x	4.53	4.50	3.20
PTO cylinder velocity	$\dot{x}$	3.79	3.76	2.47
PTO cylinder Force	$u(t)$	4.33	4.30	2.47

Case study 2: Coupled numerical wave tank and PTO models

Based on a generic, reactively controlled, HPA-type WEC (see Figure 2b), this case study will investigate the influence of different levels of model fidelity of the hydrodynamic, as well as the PTO model. To that end, four different numerical models are considered: (1) a CNWT coupled with a high–fidelity wave-to-wire (W2W) model (CNWT+W2W); (2) a CNWT coupled with an idealised, linear spring–damper PTO model (CNWT+iPTO); (3) a linear BNWT coupled with an idealised, linear spring–damper PTO model (BNWT+iPTO); (4) a non-linear BNWT with a drag coefficient of $C_d = 1$ coupled with an idealised, linear spring–damper PTO model (nlBNWT$_{C_d=1}$+W2W).

Results. The time–average absorbed and generated power values from the numerical models (2)–(4) are compared against the values from the CNWT+W2W. Absorbed power refers to the mechanical power directly absorbed from ocean waves, while generated power refers to the final electric power output. Since the CNWT+W2W accounts for all relevant hydrodynamic non-

linearities, as well as the occurring non-linearities in the PTO drivetrain, this model is considered as the benchmark in this case study.

For a quantitative comparison, Table 2 shows that the relative deviation, ε, between the CNWT+W2W model and models (2)–(4) in absorbed power. Considering only the time– average, absorber power, relatively small differences ($\varepsilon < 8\%$) can be observed between models (1), (2), and (4), indicting a sufficient accuracy of the non–linear BNWT with a drag coefficient of $C_d = 1$. Larger deviations can be observed between the linear BNWT, model (3), and the benchmark, model (1). This indicates that a linear hydrodynamic model is not able to capture all relevant hydrodynamic effects.

Considering the generated power for the comparison between the numerical models, the influence of the non–linear W2W model becomes visible. For the two numerical models including an idealised, linear, spring-damper type PTO model (i.e. model (2) and (3)), relative differences to the benchmark model (1) of up to 97.52% are calculated. For the two W2W models only a difference of $\varepsilon < 3\%$ can be observed, which is consistent with the findings for the absorbed power.

Table 2: Time-averaged absorbed and generated power obtained from the CNWT+W2W model and the percentage difference (ε) to the other considered models.

Model			Reactive control P_{abs}^{av}	Reactive control P_{gen}^{av}
(1)	CNWT+W2W	[kW]	23.76	13.99
(2)	CNWT+iPTO	[ϵ (%)]	3.03	78.36
(3)	BNWT+iPTO	[ϵ (%)]	16.32	97.52
(4)	nlBNWT$_{C_d = 1}$+W2W	[ϵ (%)]	-7.60	-2.87

Conclusions

In this paper, two different case studies are presented, highlighting the importance of (consistent) high–fidelity modelling of WECs under controlled conditions. From the presented results, two main conclusions can be drawn:

1. Considering aggressive EMCSs for WEC control, driving the system further away from the assumptions in the linear hydrodynamic model, high–fidelity hydrodynamic models have to be employed for the assessment of the performance of the EMCSs. Omitting high–fidelity hydrodynamic modelling in the evaluation stage of the control design can lead to an over–prediction of the WEC performance.
2. The holistic performance of a WEC can only be evaluated in high–fidelity by means of a comprehensive W2W simulation platform, where both high–fidelity hydrodynamic and PTO models are coupled. Minor inaccuracies in either of these major stages of the W2W model can result in significant inaccuracy in generated power estimation.

Acknowledgment

This material is based upon works supported by the Science Foundation Ireland under Grant No. 13/IA/1886. The research reported in this paper was also supported by the Higher Education Excellence Program of the Ministry of Human Capacities in the frame of Water science & Disaster Prevention research area of Budapest University of Technology and Economics (BME FIKP-VÍZ)

References

[1] A. F. de O. Falcão, "Wave energy utilization: A review of the technologies," *Renewable and Sustainable Energy Reviews*, vol. 14, pp. 899–918, 2010. https://doi.org/10.1016/j.rser.2009.11.003

[2] J. V. Ringwood, G. Bacelli, and F. Fusco, "Energy-maximizing control of wave- energy converters: The development of control system technology to optimize their operation," *IEEE Control Systems*, vol. 34, pp. 30–55, 2014. https://doi.org/10.1109/MCS.2014.2333253

[3] J. W. Kim, H. Jang, A. Baquet, J. O'Sullivan, S. Lee, B. Kim, and H. Jasak, "Technical and economic readiness review of CFD-based numerical wave basin for offshore floater design," in *Proceedings of the 2016 Offshore Technology Conference, Houston, TX, USA*, 2016. https://doi.org/10.4043/27294-MS

[4] M. Penalba, G. Giorgi, and J. V. Ringwood, "Mathematical modelling of wave energy converters: a review of nonlinear approaches," *Renewable and Sustainable Energy Reviews*, vol. 78, pp. 1188–1207, 2017. https://doi.org/10.1016/j.rser.2016.11.137

[5] C. Windt, J. Davidson, and J. Ringwood, "High-fidelity numerical modelling of ocean wave energy systems: A review of computational fluid dynamics-based numerical wave tanks," *Renewable and Sustainable Energy Reviews*, vol. 93, pp. 610 – 630, 2018. https://doi.org/10.1016/j.rser.2018.05.020

[6] W. E. Cummins, "The impulse response function and ship motions," DTIC Document, Tech. Rep., 1962.

[7] G. Giorgi and J. V. Ringwood, "Computationally efficient nonlinear Froude–Krylov force calculations for heaving axisymmetric wave energy point absorbers," *Journal of Ocean Engineering and Marine Energy*, vol. 3, no. 1, pp. 21–33, February 2017. https://doi.org/10.1007/s40722-016-0066-2

[8] J. R. Morison, M. P. O'Brien, J. W. Johnson, and S. A. Schaaf, "The forces exerted by surface waves on piles," *Petroleum Trans., AIME. Vol. 189, pp. 149-157*, 1950. https://doi.org/10.2118/950149-G

[9] C. W. Hirt and B. D. Nichols, "Volume of Fluid (VOF) Method for the Dynamics of Free Boundaries," *Journal of Computational Physics*, vol. 39, pp. 201–225, 1981. https://doi.org/10.1016/0021-9991(81)90145-5

[10] E. Berberović, N. P. van Hinsberg, S. Jakirlić, I. V. Roisman, and C. Tropea, "Drop impact onto a liquid layer of finite thickness: Dynamics of the cavity evolution," *Physical Review E*, vol. 79, pp. 036306–1 – 036306–15, 2009. https://doi.org/10.1103/PhysRevE.79.036306

[11] M. Penalba, J. Davidson, C. Windt, and J. V. Ringwood, "A high-fidelity wave-to- wire simulation platform for wave energy converters: Coupled numerical wave tank and power take-off models," *Applied energy*, vol. 226, pp. 655–669, 2018. https://doi.org/10.1016/j.apenergy.2018.06.008

[12] N. Faedo, G. Scarciotti, A. Astolfi, and J. V. Ringwood, "Energy-maximising control of wave energy converters using a moment-domain representation," *Control Engineering Practice*, vol. 81, pp. 85–96, 2018. https://doi.org/10.1016/j.conengprac.2018.08.010